



Contents lists available at ScienceDirect

Seizure: European Journal of Epilepsy

journal homepage: www.elsevier.com/locate/seizure

Developmental and epileptic encephalopathy 82 (DEE82) with novel compound heterozygous mutations of GOT2 gene

Özlem Yalçın Çapan^{a,*}, Dilşad Türkdoğan^b, Sertaç Atalay^c, Hande S. Çağlayan^d^a Department of Medical Biology, Faculty of Medicine, Tekirdağ Namık Kemal University, Tekirdağ, Turkey^b Marmara University, Medical Faculty, Department of Pediatric Neurology, Turkey^c Central Research Laboratory, Tekirdağ Namık Kemal University, Tekirdağ, Turkey^d Department of Molecular Biology and Genetics, Boğaziçi University, İstanbul, Turkey

ARTICLE INFO

Keywords:

Developmental and epileptic encephalopathies
Metabolic epilepsy
Inborn error of metabolism
Malate-aspartate shuttle
Whole exome sequencing
GOT2 enzyme
Aspartate aminotransferase
Vitamin B6 therapy

ABSTRACT

Purpose: Developmental and Epileptic Encephalopathies (DEEs) are rare neurological disorders characterized by early-onset medically resistant epileptic seizures, structural brain malformations, and severe developmental delays. These disorders can arise from mutations in genes involved in vital metabolic pathways, including those within the brain. Recent studies have implicated defects in the mitochondrial malate aspartate shuttle (MAS) as potential contributors to the clinical manifestation of infantile epileptic encephalopathy. Although rare, mutations in *MDH1*, *MDH2*, *AGC1*, or *GOT2* genes have been reported in patients exhibiting neurological symptoms such as global developmental delay, epilepsy, and progressive microcephaly.

Method: In this study, we employed exome data analysis of a patient diagnosed with DEE, focusing on the screening of 1896 epilepsy-related genes listed in the HPO and ClinVar databases. Sanger sequencing was subsequently conducted to validate and assess the inheritance pattern of the identified variants within the family. The evolutionary conservation scores of the mutated residues were evaluated using the ConSurf Database. Furthermore, the impacts of the causative variations on protein stability were analyzed through I-Mutant and MuPro bioinformatic tools. Structural comparisons between wild-type and mutant proteins were performed using PyMOL, and the physicochemical effects of the mutations were assessed using Project Hope.

Results: Exome data analysis unveiled the presence of novel compound heterozygous mutations in the *GOT2* gene coding for mitochondrial glutamate aspartate transaminase. Sanger sequencing confirmed the paternal inheritance of the p.Asp257Asn mutation and the maternal inheritance of the p.Arg262Cys mutation. The affected individual exhibited plasma metabolic disturbances, including hyperhomocysteinemia, hyperlactatemia, and reduced levels of methionine and arginine. Detailed bioinformatic analysis indicated that the mutations were located within evolutionarily conserved domains of the enzyme, resulting in disruptions to protein stability and structure.

Conclusion: Herein, we describe a case with DEE82 (MIM: # 618721) with pathologic novel biallelic mutations in the *GOT2* gene. Early genetic diagnosis of metabolic epilepsies is crucial for long-term neurodevelopmental improvements and seizure control as targeted treatments can be administered based on the affected metabolic pathways.

1. Introduction

Developmental and Epileptic Encephalopathies (DEEs) are rare neurological disorders characterized by the onset of drug-resistant multiple epileptic seizures within the first years of life, and severe developmental delays and regressions [1]. Although very rare, DEE can be caused by mutations in genes involved in metabolic pathways crucial

to various cellular functions in multiple organs including the brain. In recent years, defects in the mitochondrial malate aspartate shuttle (MAS) have been reported to be presenting the clinical phenotype of infantile epileptic encephalopathy [2,3]. The MAS is a redox shuttle that has a crucial role in regulating glycolysis and lactate metabolism by translocating reducing equivalents (NADH) from the cytosol into mitochondria [4,5]. There are four enzymes and two mitochondrial carriers

* Corresponding author.

E-mail address: oycapan@nku.edu.tr (Ö.Y. Çapan).

<https://doi.org/10.1016/j.seizure.2023.11.003>

Received 9 August 2023; Received in revised form 28 October 2023; Accepted 8 November 2023

Available online 9 November 2023

1059-1311/© 2023 British Epilepsy Association. Published by Elsevier Ltd. All rights reserved.

involved in the redox balance mechanism of MAS; cytosolic and mitochondrial NAD(H)-dependent malate dehydrogenase (MDH1 and MDH2), cytosolic and mitochondrial glutamate aspartate transaminase (GOT1 and GOT2), and the two isoforms of mitochondrial aspartate-glutamate carriers (AGC1, mainly expressed in brain and AGC2, in the liver) and oxoglutarate/malate carrier (OGC) [6]. As a first step of this shuttle mechanism, cytosolic MDH1 catalyzes the reversible reduction of oxaloacetate to malate in couple with the oxidation of NADH to NAD⁺, thus regenerating NAD⁺ in the cytosol. Malate is transported to the mitochondria via OGC where malate is oxidized to oxaloacetate by mitochondrial MDH2 by utilizing the NAD/NADH cofactor system to produce NADH in the tricarboxylic acid (TCA) cycle. Then, the GOT2 enzyme converts oxaloacetate to aspartate which is transported back to the cytosol by AGC isoforms, a shuttle mechanism coupled with the influx of glutamate to mitochondria [7]. In the last step, the GOT1 enzyme catalyzes the transamination from aspartate to cytosolic 2-oxoglutarate, therefore cytosolic glutamate is produced to be utilized in the aspartate-glutamate shuttle. MAS plays a crucial role in cellular energy metabolism, functioning as a pivotal factor in NAD⁺-dependent reactions within the cytosol, particularly in processes such as the biosynthesis of serine.

The components of MAS are highly expressed in the nervous system, therefore the defects in this shuttle may lead to neurological abnormalities. Although very rare cases, patients with mutations in *MDH1*, *MDH2*, *AGC1*, or *GOT2* genes were reported to display neurological phenotypes with global developmental delay, epilepsy, and progressive microcephaly [2,3,8-12]. Early diagnosis of the mutations in the components of mitochondrial MAS is essential as the severe clinical symptoms of the patients may be manageable with supplements which are low as a result of the defects in this metabolic pathway. Karnebeek et al. identified and presented the first pathologic bi-allelic mutations in the *GOT2* gene in four patients with infantile-onset epileptic encephalopathy from three unrelated families [3]. In this study, we report the fifth case, a male patient with bi-allelic missense mutations in the *GOT2* gene inherited from healthy unrelated parents, and also detailed bioinformatic analysis of the two pathologic mutations.

2. Subjects, materials, and methods

2.1. Subjects and clinical evaluations

The male patient and his family members included in this study were recruited for the Epi25 Project. The study was approved by the Institutional Review Board for Research with Human Subjects (INAREK) of Boğaziçi University. The informed consent form was signed by the parents of the proband for participation in the study. QIAamp DNA Blood Midi Kit (Qiagen) was used to extract the genomic DNA of individuals from the peripheral blood. Detailed clinical information including developmental and epilepsy history, morphologic details, neurological findings, and metabolic test results was reported by his neurologist.

2.2. Whole exome sequencing (WES) analysis and interpretation of candidate variants

Whole-exome sequencing for the proband was performed by Epi25 consortium according to previously described protocols [13]. Bioinformatic analysis of WES data was processed by 'SEQ variant analysis software' (Genomize, Istanbul, Turkey) by aligning the sequences to reference human genomes UCSC NCBI137/hg19. Variants were filtered for destructive (frameshift, inframe insertion/deletion, initiator codon variant, splice acceptor/ donor variant, stop gained/lost) and missense variations for 1896 epilepsy-related genes described in HPO (Human Phenotype Ontology) and ClinVar [14-16]. The frequencies of putative causative variations were checked using the following population databases: 1000 genome project, ESP6500, and GnomAD Exome. Variant

pathogenicity was assessed according to the American College of Medical Genetics and Genomics (ACMG) guidelines which categorize the variants as pathogenic (P), likely pathogenic (LP), uncertain significance (VUS), likely benign (LB), and benign (B) [17]. To evaluate the effect of missense mutations on the structure and function of the protein, *in silico* prediction tools Polyphen2, SIFT, Mutation Taster, DANN, and CADD (Combined Annotation Dependent Depletion) scores were used [18-22].

2.3. Sanger sequencing and co-segregation analysis

Sanger Sequencing was carried out for the proband and his family members to confirm and follow the co-segregation of causative variations with the disease phenotype within the family. Exon 7 of the *GOT2* gene including both causative variations was amplified by the polymerase chain reaction (PCR) by using the following primers: Forward: 5'-TGCTCTCGTGAGTCCTGGGTAT-3' and Reverse: 5'-GTCITTCATCT-TAGGGTAGGGAGG-3'. Sanger sequencing of the PCR products was performed by Eurofins Genomics' DNA sequencing service (<http://www.eurofins.com/genomic-services/>) and Chromas 2.6.6 (<http://technelysium.com.au/wp/chromas/>) was used to analyze the sequencing data.

2.4. Predicting effects of the p.Asp257Asn and p.Arg262Cys mutations on the GOT2 protein stability

The effect of the two amino acid substitutions on protein stability was tested by using I-Mutant 2.0 (<https://folding.biofold.org/i-mutant/i-mutant2.0.html>) and MUpro (<http://mupro.proteomics.ics.uci.edu>) web tools. The I-Mutant uses support vector machine (SVM) based algorithms to calculate Gibbs free energy changes (DDG) [23]. The MUpro determines the DDG using SVM and Neural Network-based algorithms [24]. Negative DDG values indicate a decrease in protein stability and positive values indicate an increase in protein stability. The MUpro was used for the validation of I-Mutant results.

2.5. Phylogenetic conservation analysis

The degree of evolutionary conservation of every amino acid of the GOT2 protein was determined using the ConSurf Database [25]. The ConSurf calculates a conservation score for each amino acid of the protein with an algorithm that analyzes the phylogenetic relation between homologous sequences. The conservation scores range from 1 (variable) to 9 (most conserved). Additionally, the ConSurf categorizes the residues as functional or structural and buried or exposed [26].

2.6. Analysis of physicochemical effects of the mutations with project hope

The Project Hope [27] server was used to analyze the physicochemical effects of the p.Asp257Asn and p.Arg262Cys mutations. The charge, size, and hydrophobicity changes caused by mutations in protein structure were predicted by the HOPE server. The GOT2 protein (UniProt ID: P00505) amino acids sequence obtained from UniProt [28] was used as input.

2.7. Visualization of the p.Asp257Asn and p.Arg262Cys mutations in 3-D GOT2 structure

The GOT2 protein structure (PDB ID: 5AX8-Chain A) was obtained from RCSB PDB (<https://www.rcsb.org/>) [29]. The PyMOL v.2.5.0 (The PyMOL Molecular Graphics System, Version 2.0 Schrödinger, LLC) software was used to visualize the protein structure. The amino acid substitutions were performed using the PyMOL mutagenesis wizard. Polar contacts, hydrophobic changes, and the electrostatic surface of the GOT2 protein variants were visualized using the software. The electrostatic surface potential of the protein variants was calculated by the

Adaptive Poisson-Boltzmann Solver (APBS) [30] plugin in PyMOL. Hydrophobic surfaces were colored by using the Python script “Color_h” (https://pymolwiki.org/index.php/Color_h).

3. Results

3.1. Clinical history of the proband and variant analysis

Male patient 12EE35 who is currently 29 years old was born from unrelated healthy parents. The onset of his first focal seizures was at the age of 3 months old. He exhibited infantile spasms when he was 7.5 months old and generalized tonic-clonic seizures at the age of 2. Developmental delays in gross -fine motor, speech, and cognition functions were recorded when seizures started. Currently, he has severe spastic tetraplegia, profound intellectual disability, and behavioral problems including self-mutilation and severe autistic traits with a lack of eye contact and verbal or nonverbal communication (Table 1). The electroencephalogram (EEG) showed diffuse severe slowing of background associated with bilateral frontal and generalized interictal epileptogenic potentials and frequent subclinical generalized tonic ictal pattern.

The biochemical profile of the blood indicated high plasma lactate and homocysteine levels and low ALT (alanine transaminase), methionine, and asparagine levels (Table 1).

Filtering of WES data for destructive and missense mutations in epilepsy-related genes revealed that the proband 12EE35 carries

Table 1
Clinical and metabolic features of the patient.

| Clinical features | |
|--|---|
| Sex | Male |
| Gestational age | 39 weeks |
| Head circumference at birth | unknown |
| Birth weight | 1600 g |
| Neonatal seizures | – |
| Uneventful neonatal period | + |
| Head circumference | 47 cm (–5.46 SD) |
| Height | 140 cm (–5.1 SD) |
| Weight | 21 kg (–5.7 SD) |
| Tone | Increased |
| Dysmorphic features | Triangle face; retrognathia; severe acquired microcephaly |
| Age of seizure onset | 3 months |
| Type of seizures | Epileptic spasms, tonic, myoclonic, atypical absence, generalized tonic-clonic seizure, focal epilepsy, status epilepticus |
| Movement disorders other than cerebral palsy | – |
| Behavioral problems | Self-mutilation and autistic features |
| Neurodevelopment problems | Profound intellectual disability |
| EEG | 1-diffuse severe background slowing 2-interictal: bilateral frontal and generalized epileptogenic potentials 3-ictal (subclinical): diffuse attenuation of background followed by low amplitude fast activity |
| Cranial MRI | Diffuse cerebral-cerebellar atrophy |
| Metabolic testing | |
| AST | 18.9 U/L (10–37 U/L) |
| ALT | 9.1 U/L (10–40 U/L) |
| Serum lactate level | >4.0 mmol/l |
| Serum ammonia | 66.4 µmol/L (Range: 16–60 µmol/L) |
| Homocysteine | 18 µmol/L (Ref. Value upper limit:15 µmol/L) |
| Vitamin B12 | 990 ng/L (Ref. Value upper limit 771 ng/L) |
| Plasma methionine | 11.7 µmol/L (Range :15–40 µmol/L) |
| Plasma asparagine | 17.7 µmol/L (Range: 37–92 µmol/L) |
| Other plasma amino acids | Normal |
| Urine organic acids | Normal |
| Serum Acylcarnitine profile | Normal |

ALT, alanine transaminase; AST, Aspartate aminotransferase; EEG, electroencephalogram; MRI, magnetic resonance imaging; SD, Standard deviation.

compound heterozygous variations in exon 7 of the *GOT2* gene (OMIM:138150): c.769G>A variation leading to the substitution of asparagine with aspartic acid at amino acid position 257 (p.Asp257Asn) and c.784C>T variation resulting in the substitution of cysteine with arginine at position 262 (p.Arg262Cys) (Table 2). We performed Sanger sequencing to confirm and follow the segregation of the causative variations in the family. As depicted in Fig. 1(a) and (b), p.Asp257Asn mutation was inherited paternally while p.Arg262Cys was inherited maternally. Both variants in the *GOT2* gene are not present in the public databases (1000 genomes/GnomAD Exome/ESP6500) and pathogenicity scores by several in silico prediction tools indicate a strong damaging effect on protein structure and function (Table 2).

3.2. Bioinformatic analysis

The MUpro and I-Mutant tools predicted that both the p.Asp257Asn and p.Arg262Cys mutations cause a decrease in the stability of the *GOT2* protein. Using the MUpro and I-Mutant tools, the DDG value for p.Asp257Asn mutation was determined as –0.470 and –1.78, respectively. The DDG value for the p.Arg262Cys mutation was estimated as –0.60 (MUpro) and –0.87 (I-Mutant). The ConSurf results revealed that Asp257 and Arg262 residues are highly conserved (Fig. 2). The ConSurf estimated the conservation score of Asp257 to be 9 and classified it as structural and buried. The conservation score of Arg262 was estimated at 8 by the ConSurf. It was additionally classified as functional and exposed. The Project HOPE server results indicated that the p.Asp257Asn and p.Arg262Cys mutations disrupt the function of the *GOT2* protein by causing changes in physicochemical properties such as charge, hydrophobicity, and size.

The p.Asp257Asn and p.Arg262Cys mutations were created using the mutagenesis wizard of PyMOL v2.5.2 on the PDB A5×8 protein model. Significant differences were determined between the H-bonds formed by wild-type and mutant residues (Fig. 3). The Asp257 (wild-type) residue formed H-bonds with three residues (Asp253, Ser251, and Gly248) (Fig. 3(a)), while Asn257 (mutant-type) was observed to form H-bonds with two residues (Asp253 and Ser251) (Fig. 3(b)). The Arg262 (wild-type) residue formed six H-bonds with five residues (Asp255, Ala258, Glu266, Leu112, and Ala113) (Fig. 3(c)) while Cys262 was observed to form three H-bonds with three residues (Ala258, Glu266, and Ile265) (Fig. 3(d)). A decrease in the number of interacting residues and H-bonds can lead to changes in protein stability and structure. These results are in agreement with the predictions of I-Mutant, MuPro, and HOPE server tools. The p.Arg262Cys mutation causes changes in hydrophobicity and electrostatic potential on the surface of the *GOT2* protein (Fig. 4). The mutant Cys262 variant (Fig. 4(b)) was observed to result in a more hydrophobic surface than the wild Arg262 variant (Fig. 4(a)). Additionally, p.Arg262Cys substitution causes the electrostatic potential on the protein surface to change from negative to positive (Fig. 4(c), (d)). As Asp257 residue is buried inside of the protein, electrostatic potential on the surface of the *GOT2* protein could not be evaluated.

4. Discussion

In recent years several mutations were reported in genes coding for the proteins that have roles in the malate-aspartate shuttle in rare cases of infantile metabolic epileptic encephalopathies. Patients harboring causative variations in the genes *GOT2*, *MDH1*, *MDH2*, and *AGC1* exhibit a comparable and overlapping phenotype characterized by abnormalities in blood metabolic profiles and manifestations in the nervous system, including intellectual disability and epilepsy.

The affected individual in this study carries bi-allelic novel mutations (p.Asp257Asn and p.Arg262Cys) in the *GOT2* gene. Both Asp257 and Arg262 residues are evolutionary highly conserved and bioinformatic analysis strongly supports the damaging effects of both substitutions on protein stability and structure. Previously homozygous p.

Table 2
Analysis of causative variations in the *GOT2* gene.

| In silico prediction analysis | | | | | | | | | | |
|-------------------------------|------------------------------------|--------|-------------|-------------------|-------------|-----------------|--------|------|------------------|--------------------|
| Causative Variation | HGVSc/ Nucleotide Change/ Location | Zygoty | Inheritance | Polyphen2 | SIFT | Mutation Taster | DANN | CADD | ACMG Scores [17] | ACMG Pathogenicity |
| p.Asp257Asn | NM_002080.4, c.769G>A, Exon 7 | HTZ | Paternal | Probably Damaging | Deleterious | Disease-causing | 0.9993 | 30 | PM2, PP3 | VUS |
| p.Arg262Cys | NM_002080.4, c.784C>T, Exon 7 | HTZ | Maternal | Probably Damaging | Deleterious | Disease-causing | 0.9992 | 32 | PM2, PP3, PM5 | LP |

ACMG, American College of Medical Genetics and Genomics; HGVSc, HTZ, Heterozygous; LP, Likely Pathogenic; PM2, Absent in population databases; PM5, Novel missense change at an amino acid residue where a different missense change determined to be pathogenic has been seen before; PP3, Multiple lines of computational evidence support a deleterious effect on the gene or gene product; VUS, Variant of Uncertain Significance.

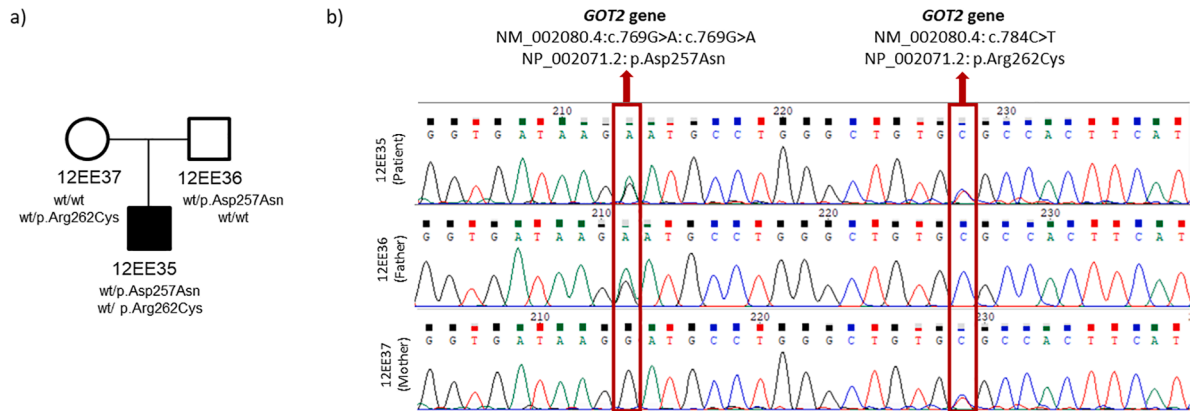


Fig. 1. Sanger sequencing and segregation analysis of the compound heterozygous mutations in the *GOT2* gene. (a) Pedigree and genotypes of the proband and family members, (b) Results of Sanger sequencing of the proband and his parents. wt; wild-type.

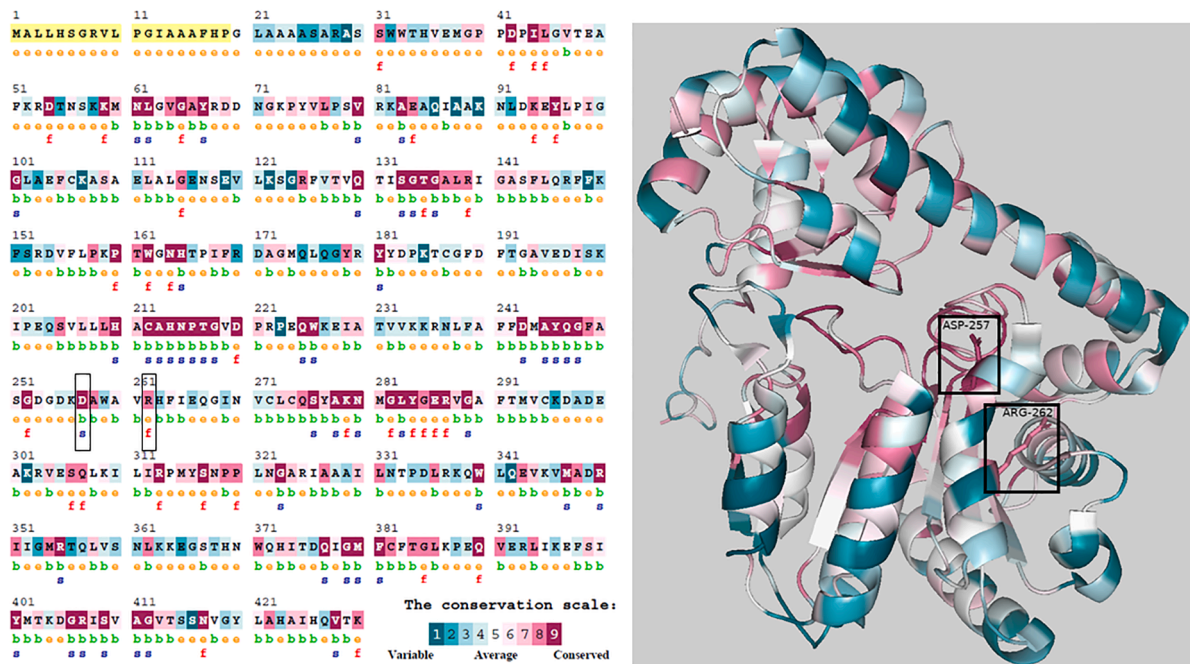


Fig. 2. The ConSurf analysis results of the *GOT2* protein. The Asp257 and Arg262 residues are enclosed in black rectangles. The 3D structure of the ConSurf results was visualized using the Pymol. The amino acids colored yellow could not be analyzed due to insufficient data. e; exposed, b; buried, f; functional, s; structural.

Arg262Gly mutation was reported in two female patients who show myoclonic and generalized tonic-clonic seizures, as well as severe intellectual and motor disability as shown in Supp. Table 1 [3]. Both female patients exhibited elevated levels of blood lactate and ammonia during metabolic screening. Our patient also has high blood lactate

levels, mild hyperammonia, hyperhomocysteine, and low levels of serum ALT, plasma asparagine, and methionine. The observed elevation in blood lactate concentrations in the affected individuals can be attributed to the impaired re-oxidation of cytosolic NADH resulting from the defective mitochondrial aspartate aminotransferase pathway.

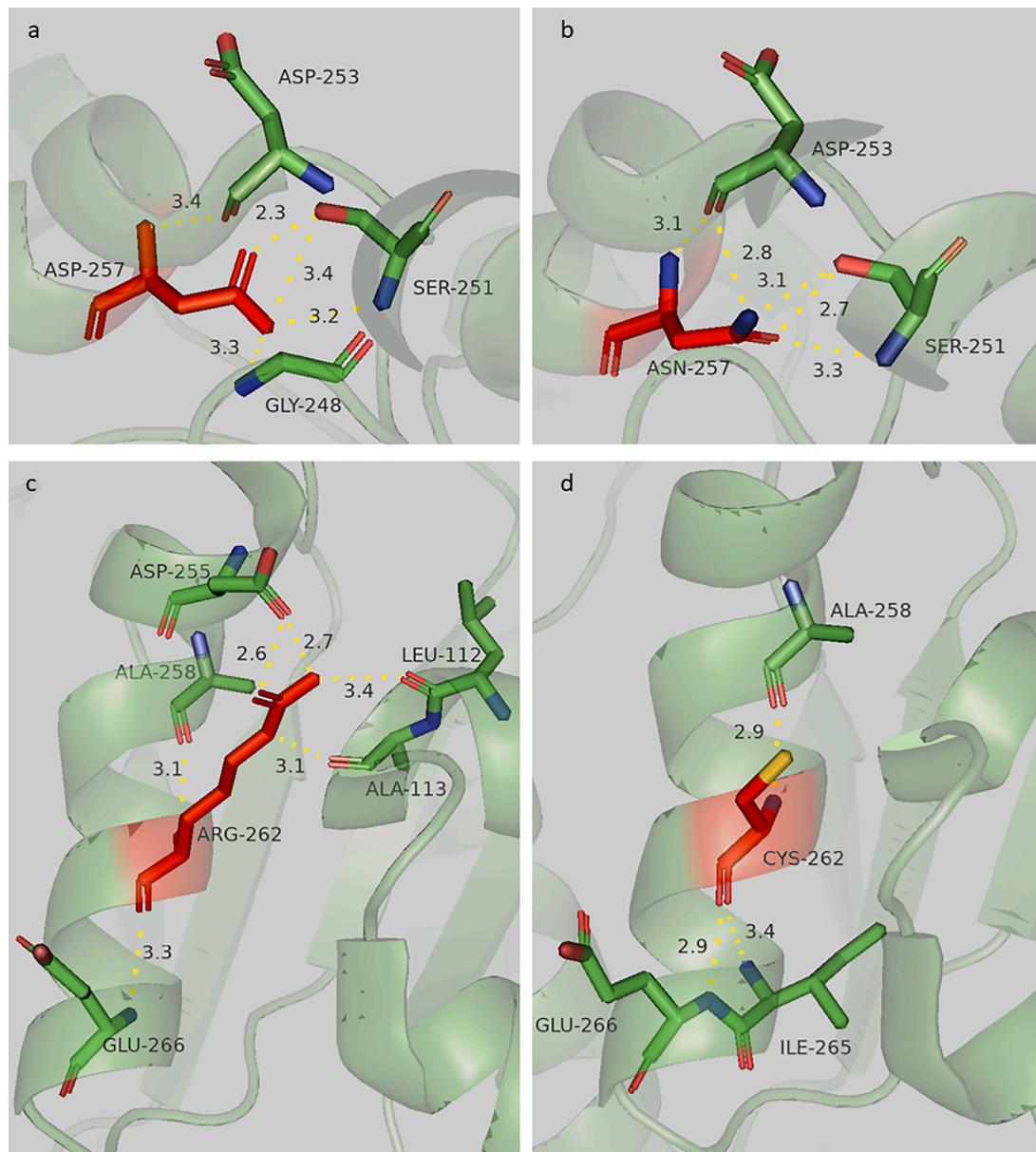


Fig. 3. 3-D comparative modeling of native and mutant residues with PyMOL v.2.5.2. (a) The five H-bonds form between Asp257 (wild-type) and Asp253 (3.4 Å), Ser251 (2.3 Å, 3.4 Å, 3.2 Å), GLY248 (3.3 Å). (b) The five H-bonds form between Asn257 (mutant-type) and Asp253 (3.1 Å and 2.8 Å), Ser251 (3.1 Å, 2.7 Å, 3.3 Å). (c) The six H-bonds form between Arg262 (wild-type) and Asp255 (2.6 Å and 2.7 Å), Ala258 (3.1 Å), Glu266 (3.3 Å), Lue112 (3.4 Å), Ala113 (3.1 Å). (d) The three H-bonds form between Cys262 (mutant-type) and Glu266 (2.9 Å), Ile265 (3.4 Å), Ala258 (2.9 Å).

Homocysteine, on the other hand, is a naturally occurring amino acid produced as part of the body's methylation process [31]. GOT2 catalyzes the reversible transfer of the amino group from aspartate to α -ketoglutarate, producing glutamate and oxaloacetate [32]. This reaction is essential for the synthesis and catabolism of amino acids, including homocysteine. Therefore, defects in the GOT2 enzyme could elucidate the deviations in the blood levels of essential amino acids.

The affected individual also has low levels of plasma methionine which serves as the precursor for homocysteine [33]. Blood levels of homocysteine and methionine are regulated through a multifaceted metabolic process that is dependent on the presence of specific B vitamins, namely folate, methylcobalamin (B12), and pyridoxal 5'-phosphate (B6). Elevated levels of plasma homocysteine can result from an excessive intake of dietary methionine or deficiencies in B vitamin levels [33]. Conversely, supplementation with B vitamins has been shown to effectively reduce plasma homocysteine concentrations. Karnebeek

et al. also reported the improved control of seizures in both zebrafish models and patients with *GOT2* gene mutations when a combination of vitamin B6 and serine is administered [3]. Therefore, our patient was also treated with vitamin B6 (250 mg/day). However, the administration of vitamin B6 was limited to a duration of merely three weeks due to the development of persistent and uncontrollable episodes of vomiting.

5. Conclusion

WES stands as a potent technological tool that has yielded a notable influence in the realm of diagnosing metabolic and neurologic disorders. The diagnostic yield of WES in the context of these conditions exhibits a broad spectrum, spanning from 16 % to 68 %, a range that has demonstrated an upward trajectory in recent years [34]. Approximately 44 % of patients have derived tangible advantages from the application of genetic diagnosis. These benefits encompass the modification of

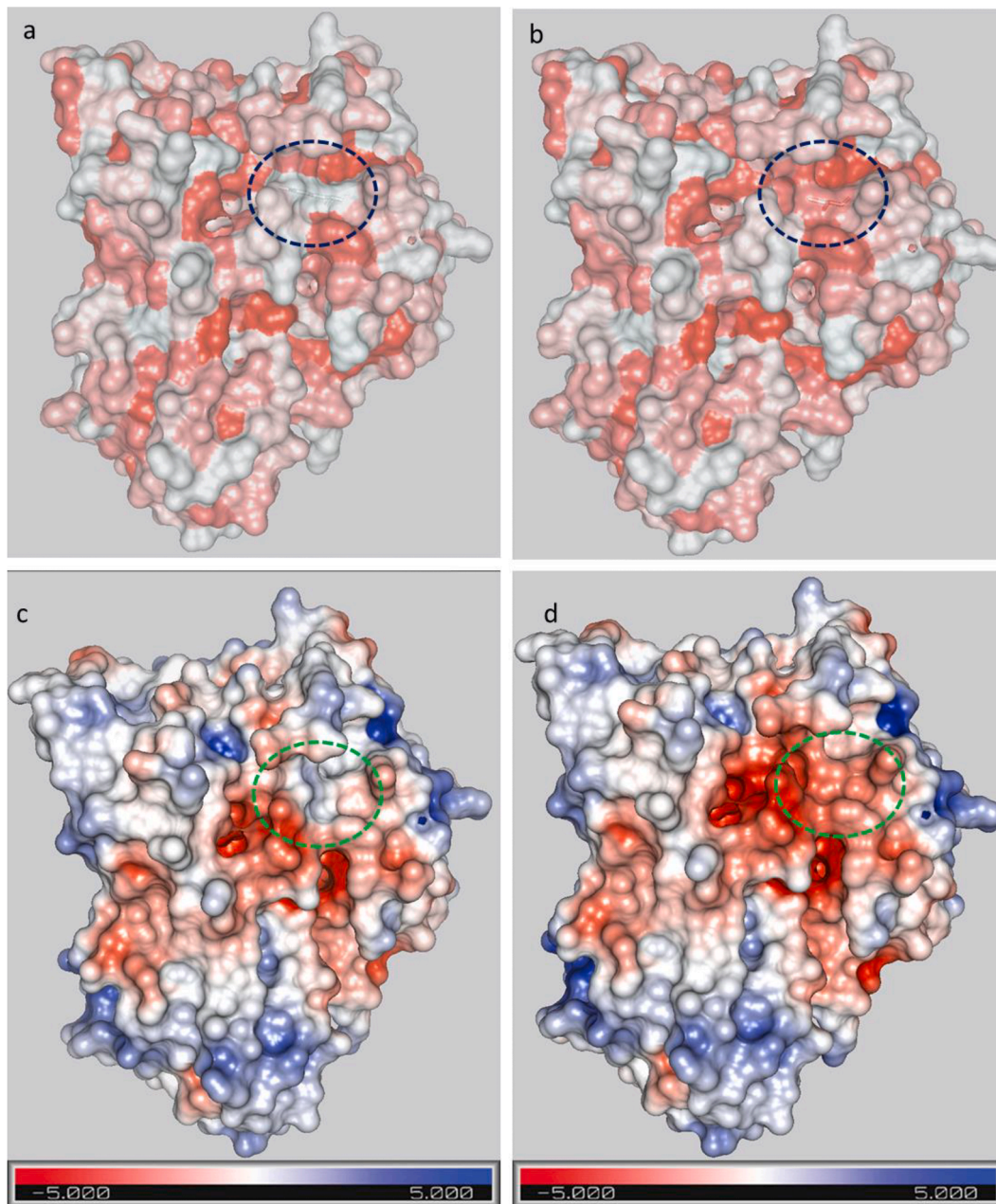


Fig. 4. Comparative modeling of hydrophobicity and electrostatic potential of the wild and mutant GOT2 protein surface with PyMOL v2.5.0. Red represents the most hydrophobic regions and white represents the most hydrophilic regions in the figures a-b. The electrostatic surface potential of wild-type and mutant GOT2 are colored ranges from -5 kT/e (red) to $+5$ kT/e (blue) according to the bar at the bottom. (a) The position of the Arg262 residue is circled in dark blue. (b) The position of the Cys262 residue is circled in dark blue. (c) The position of the Arg262 residue is circled in green. (d) The position of the Cys262 residue is circled in green. (For interpretation of the references to color in this figure legend, the reader is referred to the web version of this article.)

therapeutic protocols, the implementation of preventive interventions, and also prenatal diagnostic strategies within the family of the affected patient.

Declaration of Competing Interest

The authors declare that they have no conflict of interest.

Acknowledgments

The research project was funded by Boğaziçi University (BAP no: 17B01P3-12776).

Supplementary materials

Supplementary material associated with this article can be found, in the online version, at [doi:10.1016/j.seizure.2023.11.003](https://doi.org/10.1016/j.seizure.2023.11.003).

References

- [1] Hamdan FF, et al. High rate of recurrent de novo mutations in developmental and epileptic encephalopathies. *Am J Hum Genet* 2017;101(5):664–85. <https://doi.org/10.1016/j.ajhg.2017.09.008>.
- [2] Broeks MH, van Karnebeek CDM, Wanders RJA, Jans JJM, Verhoeven-Duif NM. Inborn disorders of the malate aspartate shuttle. *J Inher Metab Dis* 2021;44(4): 792–808. <https://doi.org/10.1002/jimd.12402>.

- [3] van Karnebeek CDM, et al. Bi-allelic GOT2 mutations cause a treatable malate-aspartate shuttle-related encephalopathy. *Am J Hum Genet* 2019;105(3):534–48. <https://doi.org/10.1016/j.ajhg.2019.07.015>.
- [4] Pardo B, Herrada-Soler E, Satrústegui J, Contreras L, Del Arco A. AGC1 deficiency: pathology and molecular and cellular mechanisms of the disease. *Int J Mol Sci* 2022;23(1):528. <https://doi.org/10.3390/ijms23010528>.
- [5] Borst P. The malate-aspartate shuttle (Borst cycle): how it started and developed into a major metabolic pathway. *IUBMB Life* 2020;72(11):2241–59. <https://doi.org/10.1002/iub.2367>.
- [6] Amoedo ND, Punzi G, Obre E, Lacombe D, De Grassi A, Pierri CL, Rossignol R. AGC1/2, the mitochondrial aspartate-glutamate carriers. *Biochim Biophys Acta* 2016;1863(10):2394–412. <https://doi.org/10.1016/j.bbamcr.2016.04.011>.
- [7] Birsoy K, Wang T, Chen WW, Freinkman E, Abu-Remaileh M, Sabatini DM. An essential role of the mitochondrial electron transport chain in cell proliferation is to enable aspartate synthesis. *Cell* 2015;162(3):540–51. <https://doi.org/10.1016/j.cell.2015.07.016>.
- [8] Pfeiffer B, Sen K, Kaur S, Pappas K. Expanding phenotypic spectrum of cerebral aspartate-glutamate carrier isoform 1 (AGC1) deficiency. *Neuropediatrics* 2020;51(2):160–3. <https://doi.org/10.1055/s-0039-3400976>.
- [9] Kavanaugh BC, Warren EB, Baytas O, Schmidt M, Merck D, Buch K, Liu JS, Phornphutkul C, Caruso P, Morrow EM. Longitudinal MRI findings in patient with SLC25A12 pathogenic variants inform disease progression and classification. *Am J Med Genet A* 2019;179(11):2284–91. <https://doi.org/10.1002/ajmg.a.61322>.
- [10] Ait-El-Mkadem S, et al. Mutations in MDH2, encoding a krebs cycle enzyme, cause early-onset severe encephalopathy. *Am J Hum Genet* 2017;100(1):151–9. <https://doi.org/10.1016/j.ajhg.2016.11.014>.
- [11] Falk MJ, et al. AGC1 Deficiency causes infantile epilepsy, abnormal myelination, and reduced N-acetylaspartate. *JIMD Rep* 2014;14:77–85. <https://doi.org/10.1007/8904.2013.287>.
- [12] Wibom R, Lasorsa FM, Töhönen V, Barbaro M, Sterky FH, Kucinski T, Naess K, Jonsson M, Pierri CL, Palmieri F, Wedell A. AGC1 deficiency associated with global cerebral hypomyelination. *New Engl J Med* 2009;361(5):489–95. <https://doi.org/10.1056/NEJMoa0900591>.
- [13] Epi25 Collaborative. Ultra-rare genetic variation in the epilepsies: a whole-exome sequencing study of 17,606 individuals. *Am J Hum Genet* 2019;105(2):267–82. <https://doi.org/10.1016/j.ajhg.2019.05.020>.
- [14] Çapan ÖY, Yapıcı Z, Özbil M, Çağlayan HS. Exome data of developmental and epileptic encephalopathy patients reveals de novo and inherited pathologic variants in epilepsy-associated genes. *Seizure* 2023. <https://doi.org/10.1016/j.seizure.2023.06.009>.
- [15] Köhler S, et al. The human phenotype ontology in 2021. *Nucleic Acids Res* 2021;49(D1):D1207–17. <https://doi.org/10.1093/nar/gkaa1043>.
- [16] Landrum MJ, Lee JM, Riley GR, Jang W, Rubinstein WS, Church DM, Maglott DR. ClinVar: public archive of relationships among sequence variation and human phenotype. *Nucl Acids Res* 2014;42(Database issue):D980–5. <https://doi.org/10.1093/nar/gkt1113>.
- [17] Richards S, Aziz N, Bale S, Bick D, Das S, Gastier-Foster J, Grody WW, Hegde M, Lyon E, Spector E, Voelkerding K, Rehm HL, ACMG Laboratory Quality Assurance Committee. Standards and guidelines for the interpretation of sequence variants: a joint consensus recommendation of the American College of Medical Genetics and Genomics and the Association for Molecular Pathology. *Genet Med* 2015;17(5):405–24. <https://doi.org/10.1038/gim.2015.30>.
- [18] Rentzsch P, Witten D, Cooper GM, Shendure J, Kircher M. CADD: predicting the deleteriousness of variants throughout the human genome. *Nucl Acids Res* 2019;47(D1):D886–94. <https://doi.org/10.1093/nar/gky1016>.
- [19] Quang D, Chen Y, Xie X. DANN: a deep learning approach for annotating the pathogenicity of genetic variants. *Bioinformatics* 2015;31(5):761–3. <https://doi.org/10.1093/bioinformatics/btu703>.
- [20] Schwarz JM, Cooper DN, Schuelke M, Seelow D. MutationTaster2: mutation prediction for the deep-sequencing age. *Nat Methods* 2014;11(4):361–2. <https://doi.org/10.1038/nmeth.2890>.
- [21] Sim NL, Kumar P, Hu J, Henikoff S, Schneider G, Ng PC. SIFT web server: predicting effects of amino acid substitutions on proteins. *Nucl Acids Res* 2012;40(Web Server issue):W452–7. <https://doi.org/10.1093/nar/gks539>.
- [22] Adzhubei IA, Schmidt S, Peshkin L, Ramensky VE, Gerasimova A, Bork P, Kondrashov AS, Sunyaev SR. A method and server for predicting damaging missense mutations. *Nat Methods* 2010;7(4):248–9. <https://doi.org/10.1038/nmeth0410-248>.
- [23] Bava KA, Gromiha MM, Uedaira H, Kitajima K, Sarai A. ProTherm, version 4.0: thermodynamic database for proteins and mutants. *Nucl Acids Res* 2004;32(Database issue):D120–1. <https://doi.org/10.1093/nar/gkh082>.
- [24] Cheng J, Randall A, Baldi P. Prediction of protein stability changes for single-site mutations using support vector machines. *Proteins* 2006;62(4):1125–32. <https://doi.org/10.1002/prot.20810>.
- [25] Ben Chorin A, Masrati G, Kessel A, Narunsky A, Sprinzak J, Lahav S, Ashkenazy H, Ben-Tal N. ConSurf-DB: an accessible repository for the evolutionary conservation patterns of the majority of PDB proteins. *Protein science: a publication of the Protein Soc* 2020;29(1):258–67. <https://doi.org/10.1002/pro.3779>.
- [26] Armon A, Graur D, Ben-Tal N. ConSurf: an algorithmic tool for the identification of functional regions in proteins by surface mapping of phylogenetic information. *J Mol Biol* 2001;307(1):447–63. <https://doi.org/10.1006/jmbi.2000.4474>.
- [27] Venselaar H, Te Beek TA, Kuipers RK, Hekkelman ML, Vriend G. Protein structure analysis of mutations causing inheritable diseases. An e-Science approach with life scientist friendly interfaces. *BMC Bioinform* 2010;5:48:11. <https://doi.org/10.1186/1471-2105-11-548>.
- [28] UniProt Consortium. UniProt: a worldwide hub of protein knowledge. *Nucl Acids Res* 2019;47(D1):D506–15. <https://doi.org/10.1093/nar/gky1049>.
- [29] Berman HM, Battistuz T, Bhat TN, Bluhm WF, Bourne PE, Burkhardt K, Feng Z, Gilliland GL, Iype L, Jain S, Fagan P, Marvin J, Padilla D, Ravichandran V, Schneider B, Thanki N, Weissig H, Westbrook JD, Zardocki C. The protein data bank. *Acta Crystallogr D* 2002;58(Pt 6 No 1):899–907. <https://doi.org/10.1107/s0907444902003451>.
- [30] Baker NA, Sept D, Joseph S, Holst MJ, McCammon JA. Electrostatics of nanosystems: application to microtubules and the ribosome. *Proc Natl Acad Sci USA* 2001;98(18):10037–41. <https://doi.org/10.1073/pnas.181342398>.
- [31] Kumar A, Palfrey HA, Pathak R, Kadowitz PJ, Gettys TW, Murthy SN. The metabolism and significance of homocysteine in nutrition and health. *Nutr Metab* 2017;14:78. <https://doi.org/10.1186/s12986-017-0233-z>.
- [32] Mellis AT, Misko AL, Arjune S, Liang Y, Erdélyi K, Ditrói T, Kaczmarek AT, Nagy P, Schwarz G. The role of glutamate oxaloacetate transaminases in sulfite biosynthesis and H2S metabolism. *Redox Biol* 2021;38:101800. <https://doi.org/10.1016/j.redox.2020.101800>.
- [33] Troen AM, Lutgens E, Smith DE, Rosenberg IH, Selhub J. The atherogenic effect of excess methionine intake. *Proc Natl Acad Sci USA* 2003;100(25):15089–94. <https://doi.org/10.1073/pnas.2436385100>.
- [34] Shakiba M, Keramatipour M. Effect of whole exome sequencing in diagnosis of inborn errors of metabolism and neurogenetic disorders. *Iran J Child Neurol* 2018;12(1):7–15.